April 30, 2021

Detecting natural selection in trait-trait coevolution

Daohan Jiang and Jianzhi Zhang*

Department of Ecology and Evolutionary Biology, University of Michigan, Ann Arbor, Michigan 48109, USA

*Correspondence to
Jianzhi Zhang
Department of Ecology and Evolutionary Biology
University of Michigan
4018 Biological Sciences Building
1105 North University Avenue
Ann Arbor, MI 48109, USA
Phone: 734-763-0527
Fax: 734-763-0544
Email: jianzhi@umich.edu

Running title: Selection in trait-trait coevolution

Keywords: fly, morphology, mutation, modularity, pleiotropy, yeast

ABSTRACT

No phenotypic trait evolves independently of all other traits, but the cause of trait-trait coevolution is poorly understood. While the coevolution could arise simply from pleiotropic mutations that simultaneously affect the traits concerned, it could also result from multivariate natural selection favoring certain trait relationships. To gain a general mechanistic understanding of trait-trait coevolution, we examine the evolution of 220 cell morphology traits across 16 natural strains of the yeast *Saccharomyces cerevisiae* and the evolution of 24 wing morphology traits across 110 fly species of the family Drosophilidae, along with the variations of these traits among gene deletion or mutation accumulation lines (a.k.a. mutants). For numerous trait pairs, the phenotypic correlation among evolutionary lineages differs significantly from that among mutants. Specifically, we find hundreds of cases where the evolutionary correlation between traits is strengthened or reversed relative to the mutational correlation, which, according to our population genetic simulation, is likely caused by multivariate selection. Furthermore, we detect selection for enhanced modularity of the yeast traits analyzed. Together, these results demonstrate that trait-trait coevolution is shaped by natural selection and suggest that the pleiotropic structure of mutation is not optimal. Because the morphological traits analyzed here are chosen largely because of their measurability, our conclusion is likely general.

INTRODUCTION

Many phenotypic traits covary during evolution. For example, the logarithm of brain weight and that of body weight show a nearly perfect linear relationship across mammals (Gould, 1966; Huxley, 1972; Lande, 1979). In theory, three processes may explain such trait-trait coevolution. First, it could arise simply from pleiotropic mutations that simultaneously influence these traits with a more or less constant ratio of effects (Lande, 1980; G. P. Wagner, 1989; G. P. Wagner & Zhang, 2011). Second, trait covariation could arise from the linkage disequilibrium between genes controlling these traits (Gardner & Latta, 2007; Lande, 2007; Saltz, Hessel, & Kelly, 2017; G. P. Wagner & Zhang, 2011), but such trait covariation is expected to be restricted to closely related individuals due to the deterioration of linkage disequilibrium as a result of recombination. If the linkage disequilibrium is stably maintained due to, for example, chromosomal inversion, the involved linked genes can be regarded as a supergene with mutational pleiotropy (Saltz et al., 2017). For this reason, linkage disequilibrium is negligible except for trait covariation among closely related individuals. Third, trait covariation could be a result of natural selection for particular trait relationships that are advantageous (Bolstad et al., 2015; Lande, 1979; Roff, Mostowy, & Fairbairn, 2002; Shoval et al., 2012; Sinervo & Svensson, 2002; Svensson et al., 2021).

Despite a long-standing interest in trait correlation in evolution (Lande, 1979; Saltz et al., 2017; G. P. Wagner & Altenberg, 1996), which is also referred to as phenotypic integration in the literature (Olson & Miller, 1999; Pigliucci, 2003), our understanding of the roles of mutation and selection in trait-trait coevolution remains limited. Most studies on the subject focused on a small number of traits that are physiologically or ecologically important (Kingsolver et al., 2001), such as skull anatomy characters (Fabre et al., 2020; Goswami, Smaers, Soligo, & Polly, 2014; Navalon, Marugan-Lobon, Bright, Cooney, & Rayfield, 2020; Porto et al., 2015; Simon, Machado, & Marroig, 2016; Watanabe et al., 2019), behavioral syndrome (i.e., sets of correlated behavioral traits) (Dochtermann & Dingemanse, 2013; Sih, Bell, & Johnson, 2004), and ecological or organismal traits correlated with the metabolic rate (Brown, Gillooly, Allen, Savage, & West, 2004; Glazier, 2010; Martin, 1981; Pettersen, White, & Marshall, 2016; White et al., 2019); hence, they may not provide a general, unbiased picture of trait-trait coevolution. Additionally, it is the trait correlation resulting from standing genetic variation and its effect on adaptation that have received the most attention (Agrawal & Stinchcombe, 2009; Arnold,

Burger, Hohenlohe, Ajie, & Jones, 2008; Blows & Mcguigan, 2015; Schluter, 1996; Steppan, Phillips, & Houle, 2002; Walsh & Blows, 2009; Walter, Aguirre, Blows, & Ortiz-Barrientos, 2018). But, because standing genetic variation could have been influenced by selection, the resulting trait correlation may not inform the correlation produced by mutation. Not knowing the mutational correlation hinders a full understanding of the contribution of selection.

Related to trait-trait correlation is the concept of modularity. It has been hypothesized that it is beneficial for organisms to have a modular organization such that functionally related traits belonging to the same module covary (Goswami et al., 2014; G. P. Wagner, 1999; G. P. Wagner & Altenberg, 1996; G. P. Wagner, Pavlicev, & Cheverud, 2007). Although modularity is a well-recognized feature of many trait correlation networks, the relative contribution of selection and mutational pleiotropy to modularity has not been assessed at the phenome scale (G. P. Wagner et al., 2007; Wang, Liao, & Zhang, 2010).

To gain a general mechanistic understanding of trait-trait coevolution, we study the phenotypic correlations for a large number of trait pairs at the levels of mutation and long-term evolution; natural selection is inferred when the evolutionary correlation between traits cannot be fully explained by the mutational correlation. Our primary data include 220 cell morphology traits of the budding yeast *Saccharomyces cerevisiae* that have been measured in 4817 single-gene deletion lines (Ohya et al., 2005), 89 mutation accumulation (MA) lines (for a subset of 187 traits) (Geiler-Samerotte, Zhu, Goulet, Hall, & Siegal, 2016), and 16 natural strains with clear phylogenetic relationships (Ohya et al., 2005; Yvert et al., 2013). These traits were quantified from fluorescent microscopic images of triple-stained cells and were originally chosen for study because of their measurability regardless of potential roles in evolution and adaptation (Ohya et al., 2005). Subsequent studies found that these traits are correlated with the yeast mitotic growth rate to varying extents (Ho & Zhang, 2014). Hence, these traits may be considered representatives of phenotypic traits that have different contributions to fitness. Previous analyses of these traits among natural strains unveiled signals of positive selection on individual traits (Ho, Ohya, & Zhang, 2017), but their potential coevolution has not been studied. While studying these trait pairs can offer a general picture of trait-trait coevolution, we recognize that the selection agent would be hard to identify should selection be detected because the biological functions of these traits (other than correlations with the growth rate) are generally unknown (Ho et al., 2017). To verify the generality of the findings from the yeast traits, we analyze another

dataset that includes 12 landmark vein intersections on the fly wings that have been measured in 150 MA lines of *Drosophila melanogaster* (Houle & Fierst, 2013) and 110 Drosophilid species (Houle, Bolstad, van der Linde, & Hansen, 2017). Because each intersection is described by two coordinates, which are counted as two traits, there are 24 traits in this dataset. In both datasets, we discover that the evolutionary correlation differs significantly from the mutational correlation for numerous trait pairs, revealing a role of natural selection in trait-trait coevolution. We also provide evidence for selection for enhanced modularity of the yeast traits.

RESULTS

Evolutionary correlations differ from mutational correlations for many trait pairs

To investigate if trait correlations in evolution can be fully accounted for by the correlations generated by mutation, we examined all pairs of the 220 yeast cell morphology traits previously measured. For each pair of traits, we computed the mutational correlation COR_M, defined as Pearson's correlation coefficient across 4,817 gene deletion lines (upper triangle in **Fig. 1A**, **Data S1**), and evolutionary correlation COR_E, defined as Pearson's correlation coefficient across 16 natural strains (lower triangle in **Fig. 1A**, **Data S1**) with their phylogenetic relationships (**Fig. S1**) taken into account (see Materials and Methods). Note that the original data contained 37 natural strains (Yvert et al., 2013), of which 21 belong to the "mosaic" group (Liti et al., 2009; Peter et al., 2018)—their phylogenetic relationships with other *S. cereviase* strains vary among genomic regions—so cannot be included in our analysis that requires considering phylogenetic relationships (Mendes, Fuentes-Gonzalez, Schraiber, & Hahn, 2018). For each pair of traits, a neutral distribution of COR_E was generated by simulating 1,000 times the neutral evolution of the traits under a multivariate Brownian motion model with the observed mutational (co)variance matrix M used as the mutational input, because, under neutrality, the expected evolutionary divergence along a dimension in the phenotypic space is proportional of the mutational variance along that dimension (Hohenlohe & Arnold, 2008; Lande, 1979; Lynch & Hill, 1986). A significant difference from COR_M ($P < 0.05$) was inferred when the observed COR_E falls in the left or right 2.5% tail of the null distribution of COR_E. Note that the above test has two limitations. First, it assumes that M is invariant among the natural strains examined such that a significant difference between COR_E and COR_M is caused by selection in trait-trait coevolution instead of M evolution. Second, our test cannot detect strain-specific selection on

trait correlation, because COR_E captures only the common pattern of trait correlation across the natural strains examined. Before conducting the test, we confirmed that the sampling error of our estimated M is negligible, likely because of the large number of mutants used in M estimation (**Table S1**; see Materials and Methods).

We found that the frequency distribution of COR_E across all trait pairs differs significantly from that of COR_M (**Fig. S2A**), suggesting the action of selection. Of the 24,090 trait pairs examined, 1,215 pairs (or 5.04%) showed a significantly different COR_E when compared with its neutral expectation from COR_M, at the false discovery rate (FDR) of 5% (**Table 1**, **Data S1**), indicating that natural selection has shaped the coevolution of many trait pairs. To investigate whether the above result is biased because of the use of each trait in many trait pairs, we randomly arranged the 220 traits into 110 non-overlapping pairs and counted the number of pairs with COR_E significantly different from COR_M. This was repeated 1,000 times to yield 1000 estimates of the proportion of trait pairs with significantly different COR_E and COR_M. The middle 95% of these estimates ranged from 1.82% to 9.09%, with the median estimate being 4.55%. Hence, there is no indication that using overlapping trait pairs has biased the estimate of the fraction of trait pairs with significantly different COR_E and COR_M.

We divided the 1,215 cases of significantly different COR_E and COR_M into three categories. In the first category, the trait correlation generated by mutation is strengthened by natural selection during evolution. A total of 393 trait pairs are considered to belong to this "strengthened" category (**Table 1**) because they satisfy the following criteria: COR_E and COR_M have the same sign and $|COR_E| > |COR_M|$, or COR_E and COR_M have different signs but only COR_E is significantly different from 0 (at the nominal P-value of 0.05) (**Fig. 1B**). In the second category, the trait correlation generated by mutation is weakened by natural selection during evolution. One hundred and forty-five trait pairs satisfying the following criteria are classified into this "weakened" category (**Table 1**): COR_E and COR_M have the same sign and $|COR_E| < |COR_M|$, or COR_E and COR_M have different signs but only COR_M is significantly different from 0 (**Fig. 1C**). In the last category, the trait correlation generated by mutation is reversed in sign by natural selection during evolution. Six hundred and seventy-seven trait pairs satisfying the following criteria are in this "reversed" category (**Table 1**): COR_E and COR_M have different signs and are both significantly different from 0 (**Fig. 1D**).

To assess the robustness of the selection signals detected, we repeated the above analysis using COR_M estimated from 89 mutation accumulation (MA) lines (Geiler-Samerotte et al., 2016) (**Fig. S3A**, **Data S1**). Again, the overall frequency distribution across all trait pairs differs significantly between COR_E and COR_M (**Fig. S2B**). We found that 1,718 trait pairs exhibit a significantly different COR_E from its neutral expectation (**Table 1**, **Data S1**), supporting a role of selection in the coevolution of many trait pairs. When comparing the analysis using COR_M from gene deletion lines and that using COR_M from MA lines, we found 429 trait pairs to exhibit selection signals and fall into the same category in both analyses, including 85 pairs in the "strengthened" category, 18 pairs in the "weakened" category, and 326 pairs in the "reversed" category. All of these numbers substantially exceed the corresponding expected random overlaps (3.4, 0.1, and 54.9, respectively; $P < 0.001$ based on 1000 random draws in each case), suggesting the reliability of both analyses. Although mutations in MA lines are more natural than those in gene deletion lines, the number of MA lines is much smaller than the number of gene deletion lines and only 187 of the original 220 traits were measured in the MA lines. For these reasons, we focused on the COR_M estimated from the gene deletion lines in subsequent analyses.

To examine the generality of the above yeast-based findings, we analyzed the 24 wing morphology traits of Drosophilid flies. The COR_M and COR_E have been previously estimated from 150 MA lines (Houle & Fierst, 2013) and 110 Drosophilid fly species (Houle et al., 2017), respectively (**Fig. S3B**, **Data S1**). The overall frequency distribution across all trait pairs differs significantly between COR_E and COR_M (**Fig. S2C**). Of the 276 pairs of traits, 152 showed a significantly different COR_E from its neutral expectation generated by simulating neutral evolution with the estimated COR_M (**Table 1**, **Data S1**), suggesting widespread actions of selection in the coevolution of fly wing morphology traits.

Together, these results demonstrate that, for many trait pairs, mutational and evolutionary correlations between morphological traits are more different than expected under neutrality. This observation suggests an important role of selection in shaping the strength and/or direction of trait correlation in evolution.

Effects of different selection regimes on trait-trait coevolution

The strengthened, weakened, and reversed trait correlations in evolution may have resulted from different selection regimes. Below we consider various selection regimes that could potentially explain these types of difference between COR_M and COR_E (**Fig. 2**). First, when a specific allometric relationship between two traits is selectively favored, the population mean trait values are expected to be concentrated near the fitness ridge or the optimal allometric line, resulting in a strong evolutionary correlation between the traits (i.e., a high $|COR_E|$) (**Fig. 2A**). Unless COR_M is already similar to COR_E, we expect to see strengthened or reversed COR_E depending on COR_M. Second, if there is a single fitness peak for an optimal combination of trait values and if there is sufficiently strong stabilizing selection on the optimal phenotype, the population mean phenotype should be restricted within a small range of the optimal phenotype in all directions in the phenotypic space regardless of the mutational variance. Consequently, COR_E is expected to be close to 0, which could account for a weakened evolutionary correlation relative to the mutational correlation (**Fig. 2B**). Finally, if the fitness optimum varies across lineages in a random fashion, the steady-state COR_E will be close to zero, potentially leading to the weakening of the evolutionary correlation relative to the mutational correlation (**Fig. 2C**).

To verify these predictions, we simulated the evolution of two traits. Under each parameter set, we simulated 50 independent replicate lineages and computed the correlation coefficient, or COR_E, between the traits across the replicate lineages at the end of the simulated evolution. This was repeated 200 times to obtain an empirical distribution of COR_E. To evaluate the difference between COR_M and COR_E, we examined the location of COR_M in the distribution of COR_E; a significant ($P < 0.05$) difference is inferred if COR_M is in the left or right 2.5% tail of the COR_E distribution.

As expected, in the absence of selection, the distribution of COR_E is centered around COR_M (first block in **Table 2**). When a specific allometric relationship is selectively favored, a high $|COR_E|$ always emerges regardless of the COR_M used, resulting in either strengthened or reversed evolutionary correlations ($P < 0.005$ for all parameter sets examined; the second to fifth blocks in **Table 2**). By contrast, stabilizing selection of an optimal phenotype leads to weakened correlation across replicate lineages when $|COR_M|$ is not small (sixth block in **Table 2**). Finally, when different lineages have different phenotypic optima that are randomly picked from the standard bivariate normal distribution, weakened evolutionary correlations are generally observed except when COR_M is close to zero (bottom block in **Table 2**). These results suggest

that the strengthened and reversed evolutionary correlations of yeast and fly morphological traits are likely caused by selections of allometric relationships, while the weakened correlations are likely caused by selections of individual traits either when there is a single optimal phenotype or when the optimal phenotype randomly varies among lineages.

Selection for enhanced modularity of yeast morphological traits

While all of the above analyses focused on individual trait pairs, here we ask whether the overall trait correlation across divergent lineages is stronger or weaker than that created by mutation. As a measure of the overall level of trait correlation (i.e., overall integration), we calculated the variance of eigenvalues (V_{eigen}) of the correlation matrix from divergent lineages and mutants, respectively. A greater V_{eigen} corresponds to a stronger overall correlation between traits because the eigenvalues become less evenly distributed as the absolute values of the correlation coefficients become larger (Pavlicev, Cheverud, & Wagner, 2009). However, the sample size (i.e., the number of strains) in the estimation of the correlation matrix also has an effect on V_{eigen}; a matrix estimated from a smaller sample naturally tends to have fewer positive eigenvalues and greater V_{eigen}. To control this factor, we used 1,000 control datasets generated by simulating neutral evolution to derive an empirical null distribution of V_{eigen} and examined the location of the observed V_{eigen} in this distribution (see Materials and Methods).

For the yeast traits, V_{eigen} of the observed evolutionary correlation matrix exceeds that in 90.8% of simulated datasets ($P = 0.184$ in a two-tailed test; **Table 3**), meaning that the overall evolutionary correlation between traits is not significantly different from the overall mutational correlation. For the fly traits, V_{eigen} of the evolutionary correlation matrix exceeds that in 99% of simulated datasets ($P = 0.02$ in a two-tailed test; **Table 3**), suggesting that the overall evolutionary correlation between traits is stronger than the overall mutational correlation. We also compared the overall integration between yeast and flies using $V_{eigen}/(n\text{-}1)$, where n is the number of traits examined. $V_{eigen}/(n\text{-}1)$ equals 0.204 and 0.268 for the yeast mutational and evolutionary matrices, respectively, whereas the corresponding values in flies are 0.153 and 0.190, respectively. Hence, the overall integration is substantially lower in flies than in yeast for both mutational and evolutionary matrices.

In addition to the overall level of trait correlation, we also asked whether the correlational structure of traits exhibit different levels of modularity among divergent lineages when compared

with that among mutants. To this end, we used a covariance ratio (*CR*) test (Adams, 2016) that compares covariance within and between pre-defined modules (see Materials and Methods). Specifically, we calculated *CR* for the evolutionary covariance matrix and compared it to the *CR* distribution based on 1,000 covariance matrices generated through simulations of neutral evolution. We treated the three non-overlapping categories of the yeast traits—actin traits, nucleus traits, and cell wall traits (Ohya et al., 2005)—as three modules (**Data S1**). We found that the *CR* of the evolutionary covariance matrix exceeded that of every control dataset ($P < 0.001$; **Table 3**), suggesting natural selection for increased modularity in evolution. Consistent with this result is the observation that trait pairs with significantly strengthened COR_E are enriched within modules ($P = 0.036$, randomization test), and this enrichment is particularly strong for the nucleus module ($P < 0.001$, randomization test). We did not analyze the fly data here because of the unknown modular structure of this relatively small set of traits that are all about the wing shape.

DISCUSSION

By comparing the trait-trait correlation across mutants (COR_M) with that across divergent lineages (COR_E) for 24,090 pairs of yeast cell morphology traits and 276 pairs of fly wing morphology traits, we detected the action of natural selection in trait-trait coevolution. The fraction of trait pairs showing evidence for selection is substantially higher in the fly (55.07%) than yeast (5.04%) data ($P < 10^{-4}$, chi-squared test). This is at least in part caused by a difference in statistical power, because the number of strains/species used for estimating COR_E is much greater for the fly (110) than yeast (16) data. It is likely that a much higher fraction than 5% of the yeast trait pairs are subject to selection in their coevolution. Furthermore, as mentioned, our comparison between COR_E and COR_M intends to test selection on trait correlations common among the evolutionary lineages considered. If different evolutionary lineages have different trait correlations, the COR_E estimated from all lineages may not be significantly different from COR_M even when selection occurs in some or all of the lineages. In other words, our test is expected to underestimate the proportion of trait pairs subject to selection. In our test, a null distribution of COR_E under neutrality was generated by simulating a Brownian motion with the observed *M* matrix used as mutational input. Although it is theoretically possible for non-neutral evolution to behave like a Brownian motion, this should not impact our test because it is

extremely unlikely for the non-neutral Brownian motion to follow *M*. Even under this unlikely scenario, a significant difference between COR_E and COR_M still signals selection while an equality between COR_E and COR_M may not prove neutrality. In other words, the potential non-neutral Brownian motion at most renders our test more conservative.

We demonstrated by population genetic simulation that various selection regimes can explain differences between COR_M and COR_E. In particular, strengthened or reversed COR_E relative to COR_M can occur when a specific allometric relationship is preferred, while weakened COR_E can occur under directional or stabilizing selection of individual traits. A notable difference between the simulation results and empirical observations is that the simulations tend to end up with extreme values of $|COR_E|$ (i.e., close to either 1 or 0) except in the case of neutrality, whereas the empirically observed $|COR_E|$ is usually less extreme even when COR_M and COR_E are significantly different. This is due to the fact that the simulation results usually represent steady-state correlations across lineages. That is, the mean phenotype of each lineage is at or near the corresponding optimum (if any); consequently, $|COR_E|$ is close to 1 when the optimum is a line and close to 0 when the optimum is a single combination of two trait values. However, the population mean phenotypes may not be close to their optima in some strains because of recent changes of the optima or the sparsity of mutations toward the optima, the latter of which is well known as a potential hindrance to adaptation (Agrawal & Stinchcombe, 2009; Blows & Mcguigan, 2015; Hansen & Houle, 2008; Schluter, 1996). Another possibility is the existence of a wide range of preferred allometry such that there is no strong selection for extreme $|COR_E|$. Finally, selection may not result in the preferred allometry between two traits because of the constraints from unconsidered traits (Houle, Jones, Fortune, & Sztepanacz, 2019).

While selection was detected for many trait pairs, a large fraction of trait pairs, especially in the yeast data, do not show a significant difference between COR_E and COR_M. These trait pairs may be divided into two groups. In the first group, COR_E and COR_M are actually different, but the difference is not found significant due to the limited statistical power. As mentioned, we believe that a substantial fraction of yeast trait pairs fit this category due to the relatively low statistical power for detecting the difference between COR_E and COR_M in the yeast data. In the second group, COR_E truly equals COR_M, which could result from one of the following three scenarios. First, the specific trait-trait correlation does not impact fitness so evolves neutrally. Second, the two traits have an intrinsic, immutable relationship (such as the hypothetical traits of

body size and twice the body size), so will yield equal COR_E and COR_M; this possibility can be tested by examining the correlation of the two traits across isogenic individuals that show non-heritable phenotypic variations (Geiler-Samerotte et al., 2020). The last and perhaps the most interesting scenario is that the trait-trait correlation impacts fitness and hence has driven the optimization of COR_M via a second-order selection (Hansen & Houle, 2008; Ho & Zhang, 2014; A. Wagner, 2005), such that the first-order selection of mutations that affect the two traits is no longer needed. However, the relative frequencies of these three scenarios are unknown.

In addition to pairwise trait correlations, we tested hypotheses regarding the evolution of overall phenotypic integration and modularity. In the yeast data, we observed a higher modularity across natural strains than across mutants but did not find evidence for a change of overall phenotypic integration in evolution. These results support the view of increasing modularity during evolution (Clune, Mouret, & Lipson, 2013; Goswami et al., 2014; G. P. Wagner, 1999; G. P. Wagner & Altenberg, 1996; G. P. Wagner et al., 2007) but also suggest that modularity is enhanced by both strengthening trait-trait correlations within modules and weakening trait-trait correlations across modules. As mentioned, we indeed observed an enrichment of strengthened COR_E relative to COR_M within modules. However, no enrichment of weakened COR_E between modules was detected, which may be because $|COR_M|$ between modules is already quite small, making a further reduction in correlation relatively difficult to detect statistically. In the fly data, we found evidence that natural selection has strengthened overall morphological integration, contrasting the hypothesis of a reduced integration over time (Goswami et al., 2014). One possible explanation is that the fly traits studied here are all characters of the same organ (wing) and their evolution does not represent that of the whole phenome but only one module. Another possibility is that the yeast cell morphology traits are not comparable with the fly wing morphology traits if they belong to different levels of biological organization (Zhang, 2018). However, for unicellular organisms like yeast, cellular traits are also organismal traits, so there is no strong evidence that these two sets of traits are not comparable. We did, however, found the overall integration lower for the fly than yeast traits, but whether this observation indicates a lower integration for multicellular than unicellular organisms requires analyzing more species and traits.

In this study, we compared COR_M estimated from one yeast strain (BY) with COR_E estimated from 16 different strains, under the assumption of a constant COR_M across different

365 strains. While it is a common practice to assume that the mutational architecture is more or less
366 constant during evolution and to study phenotypic evolution by comparing mutational or genetic
367 (co)variances in one species with those among different species (Ackermann & Cheverud, 2004;
368 Houle et al., 2017; Lynch, 1990), genetic variations affecting the genetic (co)variances of
369 phenotypic traits have been reported (Jerison et al., 2017; Jones, Burger, & Arnold, 2014;
370 Pavlicev et al., 2008). As discussed earlier, such genetic variations may allow second-order
371 selection of COR_M. For instance, it has been hypothesized that the optimization of mutational
372 (co)variances driven by selection for mutational robustness and/or adaptability can lead to
373 modularity (G. P. Wagner & Altenberg, 1996; G. P. Wagner et al., 2007), but this process
374 presumably takes a much longer time than is relevant to the present study. Even without second-
375 order selection, COR_M may still vary across strains merely because the pleiotropic effects of a
376 mutation may vary with the genetic background (Pavlicev & Cheverud, 2015; Svensson et al.,
377 2021). Regardless, in the future, it would be desirable to measure mutant phenotypes from
378 multiple lineages to investigate whether COR_M evolves, how rapidly it evolves, and whether its
379 evolution is largely neutral or adaptive.
380 In summary, we detected the action of natural selection in shaping trait-trait coevolution.
381 Because the traits analyzed here, especially the yeast traits, were chosen almost exclusively due
382 to their measurability, our results likely reflect a general picture of trait-trait coevolution.
383 Measuring these yeast traits in additional divergent natural strains with clear phylogenetic
384 positions could improve the statistical power and clarify whether the fraction of trait pairs whose
385 coevolution is shaped by selection is much greater than detected here. Finally, the detection of
386 selection for enhanced modularity of the yeast traits analyzed supports the hypothesis that
387 modularity is beneficial (Goswami et al., 2014; G. P. Wagner & Altenberg, 1996). The detection
388 of selection in trait-trait coevolution and selection for enhanced modularity suggests that the
389 current pleiotropic structure of mutation is not optimal. This nonoptimality could be due to the
390 weakness of the second-order selection on mutational structure and/or a high dependence of the
391 optimal mutational structure on the environment, which presumably changes frequently. Future
392 studies on how the mutational structure evolves will likely further enlighten the mechanism of
393 trait-trait coevolution.
394
395 **MATERIALS AND METHODS**

Phenotypic data

The *S. cerevisiae* cell morphology traits were previously measured by analyzing fluorescent microscopic images. Three phenotypic datasets were compiled and analyzed in this study, including (i) 220 traits measured in 4718 gene deletion lines that each lack an nonessential gene (Ohya et al., 2005), (ii) the same 220 traits measured in 37 natural strains (Yvert et al., 2013), and (iii) 187 of the 220 traits measured in 89 mutation accumulation (MA) lines (Geiler-Samerotte et al., 2016). When comparing patterns of trait correlation between two datasets, we used traits available in both datasets.

Before the analyses, we first standardized all trait values by converting each trait value to the natural log of the ratio of the original trait value to a reference. The standardized value of the *i*th trait in the *j*th strain is $\tilde{X}_{i,j} = \ln \frac{X_{i,j}}{X_{i,r}}$, where $X_{i,j}$ is the original trait value and $X_{i,r}$ is the trait value of the reference. For the gene deletion lines, the reference is the wild-type BY strain. For the MA lines, the reference is the progenitor strain used in MA. For natural strains, the reference is the same as the reference of the mutant strains to be compared with (i.e., wild-type BY or progenitor of the MA lines).

The locations of 12 vein intersections on the fly wing were previously measured in 150 MA lines of *Drosophila melanogaster* and a mutational covariance matrix was estimated (Houle & Fierst, 2013). These traits were also measured in 110 Drosophilid species and an evolutionary covariance matrix was estimated with species phylogeny taken into account (Houle et al., 2017). Both matrices are based on log-scale trait values.

Influence of the sampling error on the *M* matrix

To evaluate the influence of sampling error on the estimated *M* matrix of yeast or fly, we took samples (vectors of phenotypes) from the multivariate distribution of *M* (4,817 samples for yeast gene deletion data and 150 samples for fly MA data), estimated a covariance matrix ($\widetilde{M}$) from these samples, and calculated Pearson's correlation coefficient between the eigenvalues of *M* and $\widetilde{M}$. This was repeated 1,000 times and the distribution of the correlation coefficient was used to evaluate the potential impact of sampling error on *M*.

Comparison of mutational and evolutionary correlations

To take into account the phylogenetic relationships among yeast strains in estimating COR_E, we utilized a distance-based tree previously inferred (Peter et al., 2018) (**Fig. S1**). Strains with mosaic origins inferred in the same study (Peter et al., 2018) were removed before analysis, resulting in 16 remaining natural strains. Because the BY strain was not included in the data file in that study (Peter et al., 2018), W303, a laboratory strain closely related to BY, was chosen to represent BY. We obtained the evolutionary covariance matrix using the *ratematrix* function from the R package *geiger* (Pennell et al., 2014; Revell, Harmon, Langerhans, & Kolbe, 2007), which calculates evolutionary covariances using the independent contrast method (Felsenstein, 1985). The evolutionary covariance matrix was then converted to the corresponding correlation matrix.

To test whether there exists a significant modular structure among traits, we performed the covariance ratio (*CR*) test. For each pair of predefined modules, traits were first re-ordered such that traits belonging to each module were located in the upper-left and lower-right corners of the covariance matrix, respectively, and $CR = \sqrt{\frac{trace(M_{12}M_{21})}{\sqrt{trace(M_{11}^{*}M_{11}^{*})+trace(M_{22}^{*}M_{22}^{*})}}}$, where M_{12} and M_{21} are the upper-right and lower-left sections of the original covariance matrix, respectively, containing all between-module covariances, M_{11}^{*} is the upper-left section with diagonal elements replaced by zeros, M_{22}^{*} is the lower-right section with diagonal elements replaced by zeros, and $trace(M)$ denotes the trace, or the sum of diagonal elements, of matrix M (Adams, 2016). Because three modules were defined in the yeast data, the average of all pairwise *CR* values was used to represent the overall modularity.

To test whether the observed pairwise trait correlations, overall phenotypic integration, or modularity at the level of evolutionary divergence are significantly different from those expected by mutation alone, we simulated neutral evolution along the phylogenetic tree that had been used in estimating COR_E. A Brownian motion model was used to simulate phenotypic evolution such that the amount of evolution in branch i is $M_i l$, where M_i is a vector sampled from the multivariate normal distribution of the mutational covariance matrix M and l is the branch length. Sampling was performed using the *rmvnorm* function in the R package *mvtnorm* (Genz, 2020). The starting value of each trait is 0 in all simulations. The phenotypic value of each strain was obtained by adding up the amount of evolution on all branches ancestral to the strain. This was repeated 1,000 times to obtain an empirical null distribution of COR_E. The null

distributions of V_{eigen} and CR were similarly obtained. In each two-tailed test, the P-value was calculated by $P = \frac{2\min(n_H, n_L)}{1000}$, where n_H is the number of simulated values of the test statistic that are higher than the observed value, n_L is the number of those that are lower than the observed value, and $\min(n_H, n_L)$ is the smaller of n_H and n_L. The P-values for pairwise trait correlations were converted to adjusted P-values following the Benjamini-Hochberg procedure (Benjamini & Hochberg, 1995) and an adjusted P-value below 0.05 indicates selection.

Computer simulation of trait-trait coevolution under selection

In each simulation, we considered a pair of traits with equal amounts of mutational variance V_M, which is set to be 0.01. The mutational covariance matrix is thus $M = \begin{bmatrix} V_M & COV_M \\ COV_M & V_M \end{bmatrix} = \begin{bmatrix} V_M & V_M COR_M \\ V_M COR_M & V_M \end{bmatrix}$, where COV_M is the mutational covariance. The number of mutations is a random Poisson variable with the mean equal to 1. The phenotypic effect of a mutation is drawn from the multivariate normal distribution of M using the *rmvnorm* function in the R package *mvtnorm* (Genz, 2020). The starting phenotype is (0, 0) in all simulations.

We considered a Gaussian fitness function $f = \exp(-\frac{D^2}{2})$, where f is the fitness and D is the distance between the current phenotype and the optimal phenotype. When there is a single fitness peak (i.e., the fitness optimum is a single point), D is the Euclidean distance defined by $\sqrt{{d_1}^2 + {d_2}^2}$, where d_1 and d_2 are the distances between the current phenotypic values of the two traits and their corresponding optima, respectively. When there is a fitness ridge (i.e., the fitness optimum is a line), D is the shortest distance from the current phenotype to the fitness ridge. The selection coefficient s equals $\frac{f}{f_a} - 1$, where f and f_a are the fitness values of the mutant and wild-type, respectively. The fixation probability of a newly arisen mutant is $P_f = \frac{1-\exp(-2s)}{1-\exp(-2N_e s)}$ in a haploid population (Kimura, 1962), where the effective population size N_e was set at 10^4. After each unit time, the phenotypic effect of each mutation is added to the population mean at a probability of $N_e P_f$; this probability is treated as 1 when $N_e P_f > 1$ or when there is no selection. Combinations of parameters used in the simulations are listed in Table 2.

In simulations where different lineages are assigned different optima, each lineage's optimum was obtained by independently drawing the optimal values of the two traits from the standard normal distribution. Before conducting simulations, we confirmed that the optima of the two traits are not correlated (correlation coefficient = 0.0882, $P = 0.5423$, *t*-test).

All analyses in this study were conducted in R (R Core Development Team, 2010).

ACKNOWLEDGEMENTS

We thank members of the Zhang lab for valuable comments. This work was supported by U.S. National Institutes of Health grant R35GM139484 to J.Z.

REFERENCES

Ackermann, R. R., & Cheverud, J. M. (2004). Detecting genetic drift versus selection in human evolution. *Proc Natl Acad Sci U S A, 101*(52), 17946-17951. doi:10.1073/pnas.0405919102

Adams, D. C. (2016). Evaluating modularity in morphometric data: challenges with the RV coefficient and a new test measure. *Methods in Ecology and Evolution, 7*(5), 565-572. doi:10.1111/2041-210x.12511

Agrawal, A. F., & Stinchcombe, J. R. (2009). How much do genetic covariances alter the rate of adaptation? *Proceedings of the Royal Society B-Biological Sciences, 276*(1659), 1183-1191. doi:10.1098/rspb.2008.1671

Arnold, S. J., Burger, R., Hohenlohe, P. A., Ajie, B. C., & Jones, A. G. (2008). Understanding the Evolution and Stability of the G-Matrix. *Evolution, 62*(10), 2451-2461. doi:10.1111/j.1558-5646.2008.00472.x

Benjamini, Y., & Hochberg, Y. (1995). Controlling the False Discovery Rate - a Practical and Powerful Approach to Multiple Testing. *Journal of the Royal Statistical Society Series B-Statistical Methodology, 57*(1), 289-300. doi:DOI 10.1111/j.2517-6161.1995.tb02031.x

Blows, M. W., & Mcguigan, K. (2015). The distribution of genetic variance across phenotypic space and the response to selection. *Molecular Ecology, 24*(9), 2056-2072. doi:10.1111/mec.13023

Bolstad, G. H., Cassara, J. A., Marquez, E., Hansen, T. F., van der Linde, K., Houle, D., & Pelabon, C. (2015). Complex constraints on allometry revealed by artificial selection on the wing of Drosophila melanogaster. *Proceedings of the National Academy of Sciences of the United States of America, 112*(43), 13284-13289. doi:10.1073/pnas.1505357112

Brown, J. H., Gillooly, J. F., Allen, A. P., Savage, V. M., & West, G. B. (2004). Toward a metabolic theory of ecology. *Ecology, 85*(7), 1771-1789. doi:Doi 10.1890/03-9000

Clune, J., Mouret, J. B., & Lipson, H. (2013). The evolutionary origins of modularity. *Proc Biol Sci, 280*(1755), 20122863. doi:10.1098/rspb.2012.2863

Dochtermann, N. A., & Dingemanse, N. J. (2013). Behavioral syndromes as evolutionary constraints. *Behavioral Ecology, 24*(4), 806-811. doi:10.1093/beheco/art002

Fabre, A. C., Bardua, C., Bon, M., Clavel, J., Felice, R. N., Streicher, J. W., . . . Goswami, A. (2020). Metamorphosis shapes cranial diversity and rate of evolution in salamanders. *Nat Ecol Evol, 4*(8), 1129-1140. doi:10.1038/s41559-020-1225-3

Felsenstein, J. (1985). Phylogenies and the Comparative Method. *American Naturalist, 125*(1), 1-15. doi:Doi 10.1086/284325

Gardner, K. M., & Latta, R. G. (2007). Shared quantitative trait loci underlying the genetic correlation between continuous traits. *Molecular Ecology, 16*(20), 4195-4209. doi:10.1111/j.1365-294X.2007.03499.x

Geiler-Samerotte, K. A., Li, S., Lazaris, C., Taylor, A., Ziv, N., Ramjeawan, C., . . . Siegal, M. L. (2020). Extent and context dependence of pleiotropy revealed by high-throughput single-cell phenotyping. *Plos Biology, 18*(8). doi:ARTN e3000836 10.1371/journal.pbio.3000836

Geiler-Samerotte, K. A., Zhu, Y. O., Goulet, B. E., Hall, D. W., & Siegal, M. L. (2016). Selection Transforms the Landscape of Genetic Variation Interacting with Hsp90. *Plos Biology, 14*(10). doi:ARTN e2000465 10.1371/journal.pbio.2000465

Genz, A. B., F.; Miwa, T.; Mi, X.; Leisch, F.; Scheipl, F.; Hothorn, T. (2020). mvtnorm: Multivariate Normal and t Distributions. R package version 1.1-0, https://CRAN.R-project.org/package=mvtnorm.

Glazier, D. S. (2010). A unifying explanation for diverse metabolic scaling in animals and plants. *Biological Reviews, 85*(1), 111-138. doi:10.1111/j.1469-185X.2009.00095.x

Goswami, A., Smaers, J. B., Soligo, C., & Polly, P. D. (2014). The macroevolutionary consequences of phenotypic integration: from development to deep time. *Philos Trans R Soc Lond B Biol Sci, 369*(1649), 20130254. doi:10.1098/rstb.2013.0254

Gould, S. J. (1966). Allometry and Size in Ontogeny and Phylogeny. *Biological Reviews, 41*(4), 587-640. doi:DOI 10.1111/j.1469-185X.1966.tb01624.x

Hansen, T. F., & Houle, D. (2008). Measuring and comparing evolvability and constraint in multivariate characters. *Journal of Evolutionary Biology, 21*(5), 1201-1219. doi:10.1111/j.1420-9101.2008.01573.x

Ho, W. C., Ohya, Y., & Zhang, J. Z. (2017). Testing the neutral hypothesis of phenotypic evolution. *Proceedings of the National Academy of Sciences of the United States of America, 114*(46), 12219-12224. doi:10.1073/pnas.1710351114

Ho, W. C., & Zhang, J. (2014). The genotype-phenotype map of yeast complex traits: basic parameters and the role of natural selection. *Mol Biol Evol, 31*(6), 1568-1580. doi:Doi 10.1093/Molbev/Msu131

Hohenlohe, P. A., & Arnold, S. J. (2008). MIPoD: a hypothesis-testing framework for microevolutionary inference from patterns of divergence. *American Naturalist, 171*(3), 366-385. doi:10.1086/527498

Houle, D., Bolstad, G. H., van der Linde, K., & Hansen, T. F. (2017). Mutation predicts 40 million years of fly wing evolution. *Nature, 548*(7668), 447-450. doi:10.1038/nature23473

Houle, D., & Fierst, J. (2013). Properties of Spontaneous Mutational Variance and Covariance for Wing Size and Shape in Drosophila Melanogaster. *Evolution, 67*(4), 1116-1130. doi:10.1111/j.1558-5646.2012.01838.x

Houle, D., Jones, L. T., Fortune, R., & Sztepanacz, J. L. (2019). Why does allometry evolve so slowly? *Integrative and Comparative Biology, 59*(5), 1429-1440. doi:10.1093/icb/icz099

Huxley, J. (1972). Problems of relative growth. 2d.

568 Jerison, E. R., Kryazhimskiy, S., Mitchell, J. K., Bloom, J. S., Kruglyak, L., & Desai, M. M.
569 (2017). Genetic variation in adaptability and pleiotropy in budding yeast. *Elife, 6*.
570 doi:10.7554/eLife.27167
571 Jones, A. G., Burger, R., & Arnold, S. J. (2014). Epistasis and natural selection shape the
572 mutational architecture of complex traits. *Nature Communications, 5*, 3709.
573 doi:10.1038/ncomms4709
574 Kimura, M. (1962). On the probability of fixation of mutant genes in a population. *Genetics, 47*,
575 713-719.
576 Kingsolver, J. G., Hoekstra, H. E., Hoekstra, J. M., Berrigan, D., Vignieri, S. N., Hill, C. E., . . .
577 Beerli, P. (2001). The strength of phenotypic selection in natural populations. *Am Nat,*
578 *157*(3), 245-261. doi:10.1086/319193
579 Lande, R. (1979). Quantitative Genetic Analysis of Multivariate Evolution, Applied to Brain -
580 Body Size Allometry. *Evolution, 33*(1), 402-416. doi:DOI 10.1111/j.1558-
581 5646.1979.tb04694.x
582 Lande, R. (1980). The Genetic Covariance between Characters Maintained by Pleiotropic
583 Mutations. *Genetics, 94*(1), 203-215.
584 Lande, R. (2007). The maintenance of genetic variability by mutation in a polygenic character
585 with linked loci (Reprinted). *Genetics Research, 89*(5-6), 373-387.
586 doi:10.1017/S0016672308009555
587 Liti, G., Carter, D. M., Moses, A. M., Warringer, J., Parts, L., James, S. A., . . . Louis, E. J.
588 (2009). Population genomics of domestic and wild yeasts. *Nature, 458*(7236), 337-341.
589 Lynch, M. (1990). The Rate of Morphological Evolution in Mammals from the Standpoint of the
590 Neutral Expectation. *American Naturalist, 136*(6), 727-741. doi:Doi 10.1086/285128
591 Lynch, M., & Hill, W. G. (1986). Phenotypic evolution by neutral mutation. *Evolution, 40*(5),
592 915-935. doi:Doi 10.2307/2408753
593 Martin, R. D. (1981). Relative Brain Size and Basal Metabolic-Rate in Terrestrial Vertebrates.
594 *Nature, 293*(5827), 57-60. doi:DOI 10.1038/293057a0
595 Mendes, F. K., Fuentes-Gonzalez, J. A., Schraiber, J. G., & Hahn, M. W. (2018). A multispecies
596 coalescent model for quantitative traits. *Elife, 7*. doi:10.7554/eLife.36482
597 Navalon, G., Marugan-Lobon, J., Bright, J. A., Cooney, C. R., & Rayfield, E. J. (2020). The
598 consequences of craniofacial integration for the adaptive radiations of Darwin's finches
599 and Hawaiian honeycreepers. *Nat Ecol Evol, 4*(2), 270-278. doi:10.1038/s41559-019-
600 1092-y
601 Ohya, Y., Sese, J., Yukawa, M., Sano, F., Nakatani, Y., Saito, T. L., . . . Morishita, S. (2005).
602 High-dimensional and large-scale phenotyping of yeast mutants. *Proceedings of the*
603 *National Academy of Sciences of the United States of America, 102*(52), 19015-19020.
604 doi:10.1073/pnas.0509436102
605 Olson, E. C., & Miller, R. L. (1999). *Morphological integration* (Pbk. ed.). Chicago: University
606 of Chicago Press.
607 Pavlicev, M., & Cheverud, J. M. (2015). Constraints Evolve: Context Dependency of Gene
608 Effects Allows Evolution of Pleiotropy. *Annual Review of Ecology, Evolution, and*
609 *Systematics, Vol 46, 46*, 413-434. doi:10.1146/annurev-ecolsys-120213-091721
610 Pavlicev, M., Cheverud, J. M., & Wagner, G. P. (2009). Measuring Morphological Integration
611 Using Eigenvalue Variance. *Evolutionary Biology, 36*(1), 157-170. doi:10.1007/s11692-
612 008-9042-7

Pavlicev, M., Kenney-Hunt, J. P., Norgard, E. A., Roseman, C. C., Wolf, J. B., & Cheverud, J. M. (2008). Genetic variation in pleiotropy: Differential epistasis as a source of variation in the allometric relationship between long bone lengths and body weight. *Evolution, 62*(1), 199-213. doi:10.1111/j.1558-5646.2007.00255.x

Pennell, M. W., Eastman, J. M., Slater, G. J., Brown, J. W., Uyeda, J. C., FitzJohn, R. G., . . . Harmon, L. J. (2014). geiger v2.0: an expanded suite of methods for fitting macroevolutionary models to phylogenetic trees. *Bioinformatics, 30*(15), 2216-2218. doi:10.1093/bioinformatics/btu181

Peter, J., De Chiara, M., Friedrich, A., Yue, J. X., Pflieger, D., Bergstrom, A., . . . Schacherer, J. (2018). Genome evolution across 1,011 Saccharomyces cerevisiae isolates. *Nature, 556*(7701), 339-344. doi:10.1038/s41586-018-0030-5

Pettersen, A. K., White, C. R., & Marshall, D. J. (2016). Metabolic rate covaries with fitness and the pace of the life history in the field. *Proceedings of the Royal Society B-Biological Sciences, 283*(1831). doi:ARTN 20160323 10.1098/rspb.2016.0323

Pigliucci, M. (2003). Phenotypic integration: studying the ecology and evolution of complex phenotypes. *Ecology Letters, 6*(3), 265-272. doi:DOI 10.1046/j.1461-0248.2003.00428.x

Porto, A., Sebastiao, H., Pavan, S. E., VandeBerg, J. L., Marroig, G., & Cheverud, J. M. (2015). Rate of evolutionary change in cranial morphology of the marsupial genus Monodelphis is constrained by the availability of additive genetic variation. *J Evol Biol, 28*(4), 973-985. doi:10.1111/jeb.12628

R Core Development Team. (2010). R: A language and environment for statistical computing.

Revell, L. J., Harmon, L. J., Langerhans, R. B., & Kolbe, J. J. (2007). A phylogenetic approach to determining the importance of constraint on phenotypic evolution in the neotropical lizard Anolis cristatellus. *Evolutionary Ecology Research, 9*(2), 261-282.

Roff, D. A., Mostowy, S., & Fairbairn, D. J. (2002). The evolution of trade-offs: Testing predictions on response to selection and environmental variation. *Evolution, 56*(1), 84-95.

Saltz, J. B., Hessel, F. C., & Kelly, M. W. (2017). Trait Correlations in the Genomics Era. *Trends in Ecology & Evolution, 32*(4), 279-290. doi:10.1016/j.tree.2016.12.008

Schluter, D. (1996). Adaptive radiation along genetic lines of least resistance. *Evolution, 50*(5), 1766-1774. doi:DOI 10.1111/j.1558-5646.1996.tb03563.x

Shoval, O., Sheftel, H., Shinar, G., Hart, Y., Ramote, O., Mayo, A., . . . Alon, U. (2012). Evolutionary trade-offs, Pareto optimality, and the geometry of phenotype space. *Science, 336*(6085), 1157-1160. doi:10.1126/science.1217405

Sih, A., Bell, A., & Johnson, J. C. (2004). Behavioral syndromes: an ecological and evolutionary overview. *Trends in Ecology & Evolution, 19*(7), 372-378. doi:10.1016/j.tree.2004.04.009

Simon, M. N., Machado, F. A., & Marroig, G. (2016). High evolutionary constraints limited adaptive responses to past climate changes in toad skulls. *Proc Biol Sci, 283*(1841). doi:10.1098/rspb.2016.1783

Sinervo, B., & Svensson, E. (2002). Correlational selection and the evolution of genomic architecture. *Heredity (Edinb), 89*(5), 329-338. doi:10.1038/sj.hdy.6800148

Steppan, S. J., Phillips, P. C., & Houle, D. (2002). Comparative quantitative genetics: evolution of the G matrix. *Trends in Ecology & Evolution, 17*(7), 320-327. doi:Pii S0169-5347(02)02505-3 Doi 10.1016/S0169-5347(02)02505-3

Svensson, E. I., Arnold, S. J., Burger, R., Csillery, K., Draghi, J., Henshaw, J. M., . . . Runemark, A. (2021). Correlational selection in the age of genomics. *Nat Ecol Evol*. doi:10.1038/s41559-021-01413-3

Wagner, A. (2005). *Robustness and evolvability in living systems*. Princeton, NJ: Princeton University Press.

Wagner, G. P. (1989). Multivariate mutation-selection balance with constrained pleiotropic effects. *Genetics, 122*(1), 223-234.

Wagner, G. P. (1999). A research programme for testing the biological homology concept. *Novartis Found Symp, 222*, 125-134; discussion 134-140.

Wagner, G. P., & Altenberg, L. (1996). Perspective: Complex Adaptations and the Evolution of Evolvability. *Evolution, 50*(3), 967-976. doi:10.1111/j.1558-5646.1996.tb02339.x

Wagner, G. P., Pavlicev, M., & Cheverud, J. M. (2007). The road to modularity. *Nature Reviews Genetics, 8*(12), 921-931. doi:10.1038/nrg2267

Wagner, G. P., & Zhang, J. Z. (2011). The pleiotropic structure of the genotype-phenotype map: the evolvability of complex organisms. *Nature Reviews Genetics, 12*(3), 204-213. doi:10.1038/nrg2949

Walsh, B., & Blows, M. W. (2009). Abundant Genetic Variation plus Strong Selection = Multivariate Genetic Constraints: A Geometric View of Adaptation. *Annual Review of Ecology Evolution and Systematics, 40*, 41-59. doi:10.1146/annurev.ecolsys.110308.120232

Walter, G. M., Aguirre, J. D., Blows, M. W., & Ortiz-Barrientos, D. (2018). Evolution of Genetic Variance during Adaptive Radiation. *American Naturalist, 191*(4), E108-E128. doi:10.1086/696123

Wang, Z., Liao, B. Y., & Zhang, J. (2010). Genomic patterns of pleiotropy and the evolution of complexity. *Proc Natl Acad Sci U S A, 107*(42), 18034-18039. doi:10.1073/pnas.1004666107

Watanabe, A., Fabre, A. C., Felice, R. N., Maisano, J. A., Muller, J., Herrel, A., & Goswami, A. (2019). Ecomorphological diversification in squamates from conserved pattern of cranial integration. *Proc Natl Acad Sci U S A, 116*(29), 14688-14697. doi:10.1073/pnas.1820967116

White, C. R., Marshall, D. J., Alton, L. A., Arnold, P. A., Beaman, J. E., Bywater, C. L., . . . Ortiz-Barrientos, D. (2019). The origin and maintenance of metabolic allometry in animals. *Nat Ecol Evol, 3*(4), 598-603. doi:10.1038/s41559-019-0839-9

Yvert, G., Ohnuki, S., Nogami, S., Imanaga, Y., Fehrmann, S., Schacherer, J., & Ohya, Y. (2013). Single-cell phenomics reveals intra-species variation of phenotypic noise in yeast. *BMC Syst Biol, 7*, 54. doi:10.1186/1752-0509-7-54

Zhang, J. Z. (2018). Neutral Theory and Phenotypic Evolution. *Molecular Biology and Evolution, 35*(6), 1327-1331. doi:10.1093/molbev/msy065

698 Table 1. Number of trait pairs with significantly different COR_E and COR_M.

	Yeast		Fly
	COR_M from gene deletion lines (24,090 trait pairs)	COR_M from MA lines (17,391 trait pairs)	(276 trait pairs)
Strengthened	393	578	57
Weakened	145	281	59
Reversed	677	859	36
Total	1215	1718	152

699
700
701

Table 2. Parameters and results of simulations of trait-trait coevolution.

Optimum	COR_M	Median COR_E at the end of simulation	Fraction of simulations with $COR_E > COR_M$	COR_E compared with COR_M
No optimum	0.9	0.900	49.5%	No difference
	0.5	0.495	47.5%	No difference
	0.1	0.113	55.5%	No difference
$y = x$ *	0.9	1.000	100%	Strengthened
	0.5	1.000	100%	Strengthened
	0.1	1.000	100%	Strengthened
$y = 0.5x$	0.9	1.000	100%	Strengthened
	0.5	1.000	100%	Strengthened
	0.1	1.000	100%	Strengthened
$y = -0.5x$	0.9	-0.995	0%	Reversed
	0.5	-0.999	0%	Reversed
	0.1	-1.000	0%	Reversed
$y = -x$	0.9	-0.997	0%	Reversed
	0.5	-0.999	0%	Reversed
	0.1	-1.000	0%	Reversed
(0, 0)	0.9	0.0213	0%	Weakened
	0.5	0.00142	0.5%	Weakened
	0.1	-0.0109	24%	No difference
Drawn from $\mathcal{N}(\mathbf{0}, \mathbf{1})$	0.9	0.0895	0%	Weakened
	0.5	0.0874	0%	Weakened
	0.1	0.0866	6%	No difference

*x and y respectively represent the values of the two traits considered.

Table 3. Overall phenotypic integration (V_{eigen}) and modularity (CR) at the levels of mutation and evolutionary divergence. Values at the level of mutation are medians from 1,000 control sets.

Statistic	Taxon	Mutation	Divergence	*P*-value
V_{eigen}	Yeast	44.814	58.656	0.186
	Fly	3.530	4.359	0.02
CR	Yeast	0.759	0.997	< 0.001

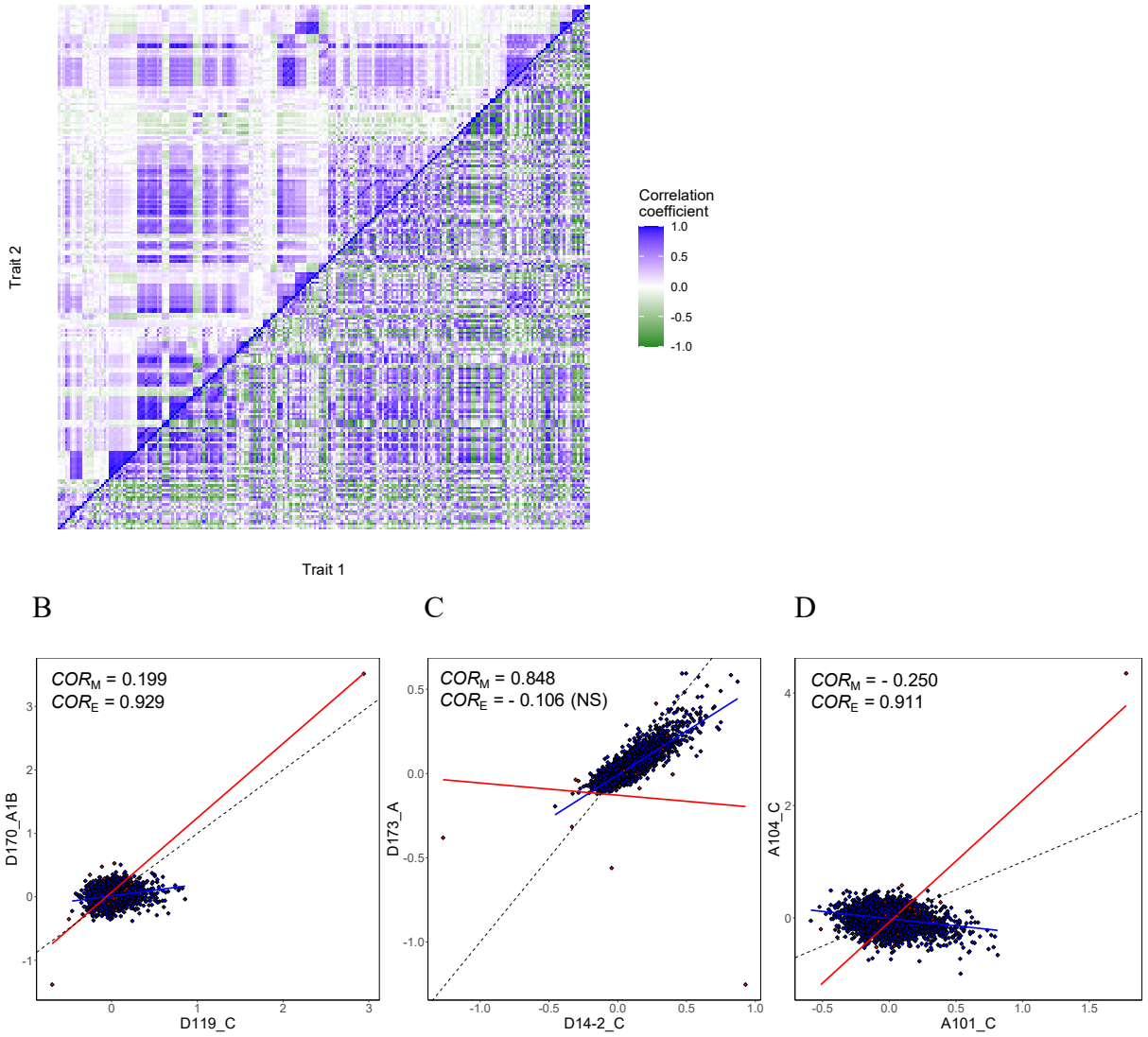

Figure 1. Detecting selection in yeast cell morphology trait-trait coevolution. (A) Mutational (COR_M, upper triangle) and evolutionary (COR_E, lower triangle) correlation matrices for the 220 yeast traits, which are ordered according to their IDs. (B) An example of evolutionarily strengthened correlation. (C) An example of evolutionarily weakened correlation. (D) An example of evolutionarily reversed correlation. In (B)-(D), each blue dot represents a gene deletion line (a.k.a. mutant) while each red dot represents an independent contrast derived from natural strains. Blue and red lines are linear regressions between the standardized values of the two traits in mutants and independent contrasts, respectively, while the dotted blackline shows the diagonal ($y = x$). Trait IDs are shown along the axes. All COR_M and COR_E values shown are significantly different from 0 except when indicated by "NS" in the parentheses.

731 A

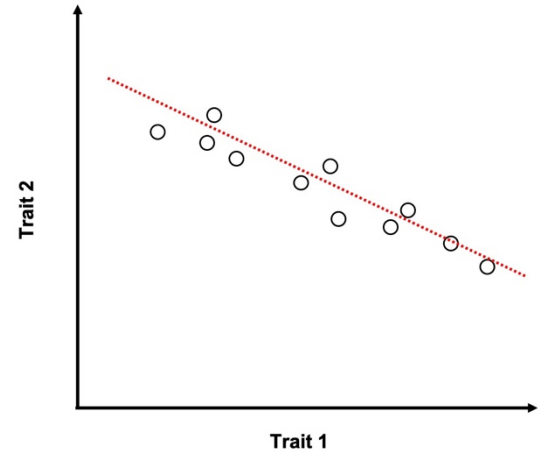

732
733 B

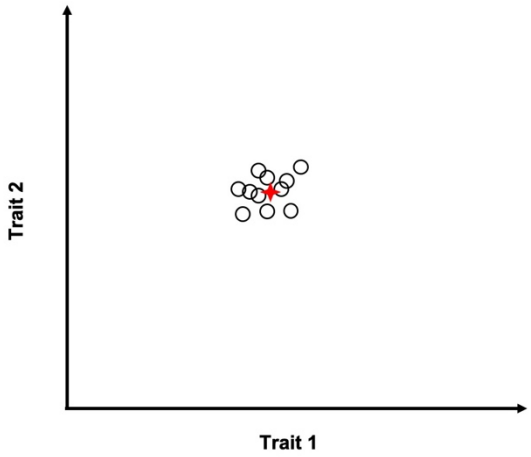

734
735 C

736
737 **Figure 2.** Schematic illustration of predictions made by models of trait-trait coevolution. Each
738 circle represents the equilibrium mean phenotype of two hypothetical traits (trait 1 and trait 2) of
739 a diverging lineage. (A) When a specific allometric relationship is selectively favored, the
740 population mean phenotypes are distributed along the fitness ridge (i.e., the optimal allometric

741 line shown in red), resulting in a strong trait correlation across lineages. (B) When a specific
742 value is selectively favored for each trait, the population mean phenotypes are concentrated near
743 the optimal phenotype (marked by the red cross) and the trait correlation across lineages is weak.
744 (C) When different lineages have different optimal phenotypes (marked by red crosses) that are
745 randomly distributed, the trait correlation across lineages is weak.

Supplementary materials for "Detecting natural selection in trait-trait coevolution"

D. Jiang & J. Zhang

The supplementary materials include:

Table S1

Figures S1-S3

Data S1 (in a separate Excel file)

Table S1. Pearson's correlation between eigenvalues of M and those of the covariance matrix estimated from samples from M ($\widetilde{M}$). Results from 1000 replicates are shown.

Taxon	Sample size	Minimum correlation coefficient	Median correlation coefficient
Yeast	4,817	0.9993745	0.9999503
Fly	150	0.9698937	0.9967839

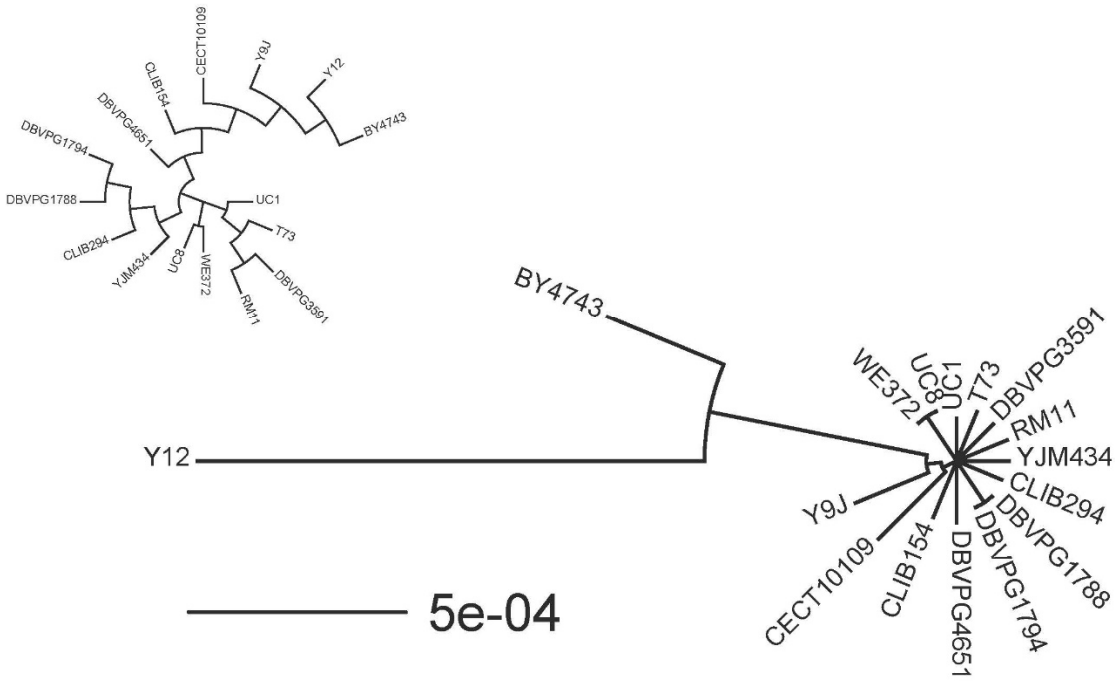

Fig. S1. Neighbor-joining tree of the 16 natural yeast strains used in this study, based on 1,544,489 biallelic single nucleotide polymorphism (SNP) sites. Scale bar indicates genomic divergence level. The tree was based on the distance matrix downloaded from http://1002genomes.u-strasbg.fr/files/1011DistanceMatrixBasedOnSNPs.tab.gz. The inset at the top left coner shows the tree topology but the branch lengths are not drawn to scale.

A

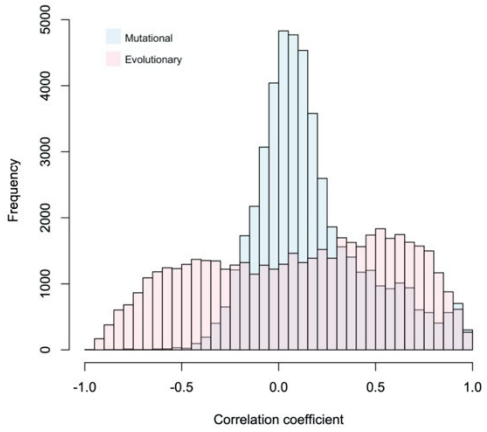

B

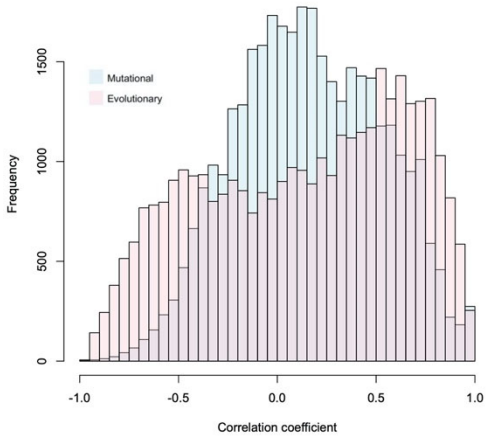

C

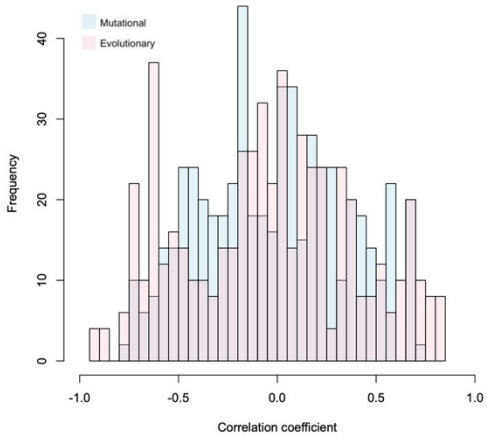

Fig. S2. Frequency distributions of multional (COR_M) and evolutionary (COR_E) correlations across all examined trait pairs. (A) Distributions for yeast when COR_M is based on gene deletion

lines. (B) Distributions for yeast when COR_M is based on MA lines. (C) Distributions for fly when COR_M is based on MA lines. The distributions for COR_M and COR_E are significantly different in each panel ($P < 10^{-10}$ in A and B and $P = 0.0015$ in C, Kolmogorov–Smirnov test).

A

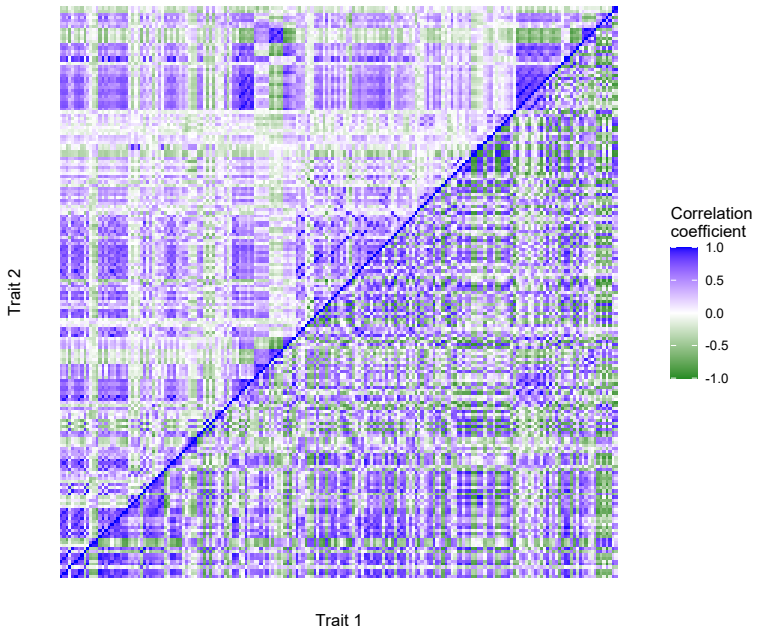

B

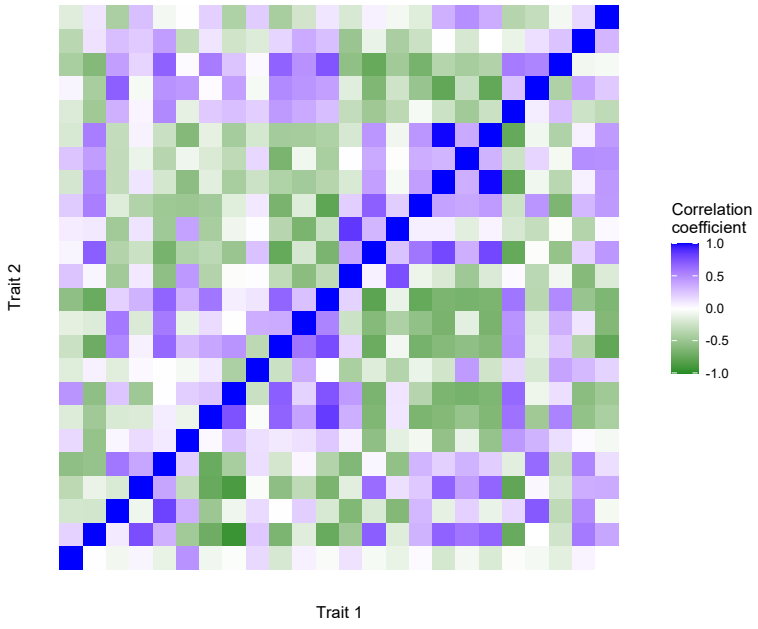

Fig. S3. Mutational (upper triangle) and evolutionary (lower triangle) correlation matrices for (A) the 187 yeast traits measured in MA lines, which are ordered according to their IDs, and (B) the 24 fly traits, which are ordered in the same way as in the original dataset.